AD-A186 140 WAVE PROPAGATION EXPERIMENTS ON 22-BAY LATTICE(U) WEA CAMBRIDGE MA J H WILLIAMS ET AL. 01 JUN 87 AFOSR-TR-87-1289 F49620-85-C-0148 1/1

UNCLASSIFIED F/G 22/2 NL

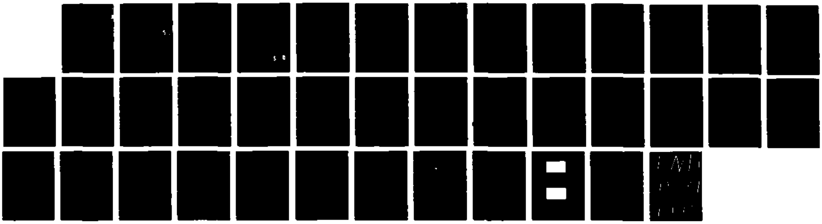

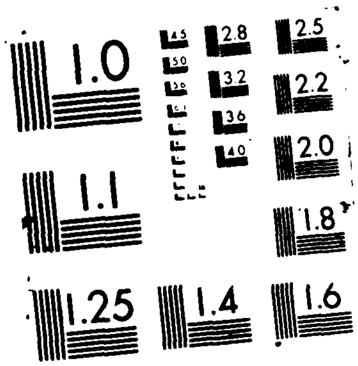
1.0
1.1
1.25
1.4
1.6
1.8
2.0
2.2
2.5
2.8
3.2
3.6
4.0

UNCLAS

SECURITY C

AD-A186 140

(2)

REPORT DOCUMENTATION PAGE

DTIC FILE COPY

1a. REPORT SECURITY CLASSIFICATION UNCLASSIFIED	1b. RESTRICTIVE MARKINGS
2a. SECURITY CLASSIFICATION AUTHORITY	3. DISTRIBUTION/AVAILABILITY OF REPORT APPROVED FOR PUBLIC RELEASE: DISTRIBUTION UNLIMITED
2b. DECLASSIFICATION/DOWNGRADING SCHEDULE	
4. PERFORMING ORGANIZATION REPORT NUMBER(S)	5. MONITORING ORGANIZATION REPORT NUMBER(S) AFOSR-TR- 87-1289
6a. NAME OF PERFORMING ORGANIZATION WEA	6b. OFFICE SYMBOL (If applicable)
7a. NAME OF MONITORING ORGANIZATION AFOSR/NA	
6c. ADDRESS (City, State and ZIP Code) P.O. Box 260, MIT Branch Cambridge, MA 02139	7b. ADDRESS (City, State and ZIP Code) Bldg 410 Bolling AFB DC 20332-6448
8a. NAME OF FUNDING/SPONSORING ORGANIZATION AIR FORCE OFFICE OF SCIENTIFIC RESEARCH	8b. OFFICE SYMBOL (If applicable) AFOSR/NA
9. PROCUREMENT INSTRUMENT IDENTIFICATION NUMBER F49620-85-0148	
8c. ADDRESS (City, State and ZIP Code) Bldg 410 BOLLING AFB, DC 20332-6448	10. SOURCE OF FUNDING NOS.
11. TITLE (Include Security Classification) WAVE PROPAGATION EXPERIMENTS ON 22-BAY LATTICE (UNCLASSIFIED)	

PROGRAM ELEMENT NO.	PROJECT NO.	TASK NO.	WORK UNIT NO.
61102F	2302	B1	

DTIC ELECTE SEP 2 9 1987 S E

12. PERSONAL AUTHOR(S) James H. Williams, Jr. and Jia J. Zhang			
13a. TYPE OF REPORT TECHNICAL	13b. TIME COVERED FROM 1 Sept 85 TO 1 June 87	14. DATE OF REPORT (Yr., Mo., Day) 1987, June, 1	15. PAGE COUNT 37
16. SUPPLEMENTARY NOTATION			

17. COSATI CODES			18. SUBJECT TERMS (Continue on reverse if necessary and identify by block number)
FIELD	GROUP	SUB. GR.	LARGE SPACE STRUCTURES; WAVE EXPERIMENTS; WAVE PROPAGATION; PERIODIC LATTICE

19. ABSTRACT (Continue on reverse if necessary and identify by block number)

Wave propagation characteristics of large space structures (LSS) affect their performance, integrity and the ability to nondestructively assess their integrity. In this study, wave propagation characteristics of an aluminum 22-bay planar lattice structure are determined experimentally. Two ultrasonic piezoceramic longitudinal transducers are mounted at various locations on the structure. Wave measurements are obtained by injecting an impulsive load via the transmitting transducer and recording the response via the receiving transducer. The waves injected into the structure are longitudinal waves, transverse to the surface, although a complex stress distribution which may be described by directivity functions is actually realized. The impulsive loading signal has a broad frequency spectrum containing frequencies greater than 0.5 MHz.

In the lattice considered, waves propagate through "T" and "L" joints into various members of the structure. The speeds of arrival of the initial waves are

20. DISTRIBUTION/AVAILABILITY OF ABSTRACT UNCLASSIFIED/UNLIMITED ☒ SAME AS RPT. ☐ DTIC USERS ☐	21. ABSTRACT SECURITY CLASSIFICATION UNCLASSIFIED
22a. NAME OF RESPONSIBLE INDIVIDUAL ANTHONY K. AMOS	22b. TELEPHONE NUMBER (Include Area Code) 202/767-4937
22c. OFFICE SYMBOL AFOSR/NA	

DD FORM 1473, 83 APR EDITION OF 1 JAN 73 IS OBSOLETE.

SECURITY CLASSIFICATION OF THIS PAGE

19. ABSTRACT (cont'd)

measured. The resulting speeds of wave propagation along members of the lattice are measured to range from 4.53 km/s (14,800 ft/s) to 5.18 km/s (17,000 ft/s). It is indicated that the measured wave speed is between the longitudinal wave speed and the flexural wave speed.

The frequency spectra of the output signals are also obtained. It is observed that the frequency at the maximum amplitude of the output spectrum generally occurs between 353 kHz and 450 kHz. It is also observed that, beyond the first five bays, the maximum amplitude of the output spectrum decreases logarithmically with the number of bays that the output is located away from the input, regardless of the input location on the structure. Thus, an attenuation of the maximum amplitude of the output spectrum can be defined for LSS based on the number of lattice bays. This attenuation parameter may be convenient for the design of LSS because it is based on a natural unit of the LSS, namely, the lattice bay. For the planar lattice considered, this attenuation is found to be 0.085 neper per bay.

Furthermore, reciprocity between input and output is observed experimentally, in both the time domain and the frequency domain. The development of quantitative measures of reciprocity is recommended.

This experimental study also demonstrates that wave propagation characteristics of a lattice structure can be obtained. In particular, the wave speed, the frequency at the maximum amplitude of the output spectrum, and the attenuation of the maximum amplitude of the output spectrum per lattice bay traversed appear to be useful parameters in the characterization of wave propagation properties of LSS. Further study should investigate the effects of boundaries, lattice member connectivities, and structural defects on these parameters. Perhaps, statistical energy analysis or pattern recognition techniques would also be of benefit in such efforts.

AFOSR-TR- 87-1289

ACKNOWLEDGEMENTS

The Air Force Office of Scientific Research (Project Monitor, Dr. Anthony K. Amos) is gratefully acknowledged for its support of this research.

Accession For		
NTIS GRA&I	☒	
DTIC TAB	☐	
Unannounced	☐	
Justification		
By		
Distribution/		
Availability Codes		
Dist	Avail and/or Special	
A-1		

QUALITY INSPECTED 2

NOTICE

This document was prepared under the sponsorship of the Air Force. Neither the US Government nor any person acting on behalf of the US Government assumes any liability resulting from the use of the information contained in this document. This notice is intended to cover WIA as well.

TABLE OF CONTENTS

LIST OF TABLES

LIST OF FIGURES

INTRODUCTION

Large space structures (LSS) are periodic lattice structures being considered for use in orbiting space stations, space communication antennas and space platforms [1]. The proposed application of LSS in geocentric orbit requires structures of outstanding performance and integrity under extreme or hostile environmental conditions. Wave propagation characteristics of LSS affect their performance, integrity and the ability to nondestructively assess their integrity in service.

Wave propagation characteristics of an aluminum 22-bay planar lattice structure[2-4] are measured experimentally in this study. Two ultrasonic piezoceramic longitudinal transducers are mounted at various locations on the structure. Wave measurements are obtained by injecting an impulsive load via the transmitting transducer and recording the response via the receiving transducer. The waves injected into the structure are generated as longitudinal waves, transverse to the surface.

In the lattice considered, waves propagate through "T" and "L" joints into various members of the structure. The resulting speeds of wave propagation along members of the lattice are measured. The frequency spectra of output signals at various locations due to input excitations at various locations on the lattice are measured also. The wave speed and the frequency spectrum should be useful in the characterization of wave propagation properties of LSS.

LATTICE GEOMETRY, EXPERIMENTAL EQUIPMENT AND EXPERIMENTAL PROCEDURES

Lattice Geometry

Fig. 1 shows the geometry of the 22-bay planar lattice structure considered in this study and in other studies [2-4]. The structure has twenty-two repeating substructures (bays). The 22-bay planar lattice is machined from a single piece of 0.953 cm (0.375 in) thick 6061-T6 aluminum plate. Thus, the structure contains no welds or fasteners in its construction.

Experimental Equipment

A schematic of the wave measurement system is shown in Fig. 2. The system consists of a broadband ultrasonic pulser-receiver (Panametrics model 5052PR) to generate and receive electrical pulses up to 30 MHz; 2.54 cm (1 in) diameter (1.91 cm (0.75 in) diameter piezoceramic element) broadband (0.1 to 3.0 MHz) transmitting and receiving longitudinal transducers (Panametrics model V105) having an approximately flat sensitivity of -85 dB (relative to 1 V/ Bar) and weighing 0.082 kgf (0.18 lbf) each; a transducer specimen interface couplant (Acoustic Emission Technology model SC-6); 26.7 N (6 lbf) constant-force springs (Acoustic Emission Technology model CFC-6.0) to secure the transducers onto the specimen; and a 16-bit digital oscilloscope (Nicolet model 4094 with dual-channel 8-bit plug-in model 4175, dual disk recorder model XF-44/2 and Waveform Analysis Package) having a maximum sampling frequency of 50 MHz (500 MHz for repetitive signals), a maximum storage capability of 15,872 data

points per trace, and a Fourier transform software package capable of handling up to 2,048 points per trace.

Experimental Procedures

The lattice as shown in Fig. 1 is suspended freely in air via two thin strings. Two transducers are attached to the lattice at various locations using the constant-force springs and are coupled to the structure via the transducer specimen interface couplant. The resulting clamping pressure of 0.11 MPa (16 psi) on the transducer is approximately equal to the saturation pressure which is defined in [5] as the minimum transducer-specimen interface pressure which results in the maximum amplitude of the output signal, all other parameters being held constant. Furthermore, the orientation of each transducer relative to the structural members of the lattice is maintained throughout to avoid any variations that could be introduced by the directional effects of the transducer piezoceramic element.

An impulse is input into the transmitting transducer via the ultrasonic pulser-receiver. The signal arriving at the receiving transducer is recorded on a 13.3 cm (5.25 in) diameter diskette using a sampling frequency of 5 MHz and 15,872 data points per trace.

The arrival time of the initial output wave signal is noted from the time trace. From this arrival time and the shortest wave path length between the transmitting and the receiving transducers through the elements of the lattice, a wave speed is calculated for the initial wave to propagate from the

transmitting transducer to the receiving transducer. Also, the frequency spectrum of the output signal is obtained via the Fast Fourier Transform (FFT), employing the Hanning window provided by the Nicolet Waveform Analysis Package using 2,048 points (initiated at the beginning of the output wave packet).

Fig. 3 shows locations A through V_1 used to locate positions on the lattice. The input is applied at locations A, L, V_C and V_1, and the output is recorded at all the remaining locations on the lattice.

Characterization of Input Pulse

The input impulse (including the transducers and the electronic equipment) is characterized by coupling the transmitting and receiving transducers directly (face-to-face) without the presence of any specimen. When the receiving transducer is coupled directly to the transmitting transducer without the structure, the output of the receiving transducer is as shown in Fig. 4a. The corresponding frequency spectrum is shown in Fig. 4b.

On the time scale being used in these experiments, there is no observable time delay between the input and the output when the transducers are coupled face-to-face as shown in Fig. 4a. In the frequency domain, as shown in Fig. 4b, the input signal contains a broad frequency spectrum from zero frequency to frequencies greater than 0.5 MHz.

RESULTS AND DISCUSSIONS

Wave Speed

The measured wave speeds for initial wave fronts arriving at various output locations for various input locations are summarized in Table 1. The measurement error of the wave speed is estimated to be less than 2 percent.

As shown in Table 1, the wave speed ranges from 4.53 km/s (14,800 ft/s) to 5.18 km/s (17,000 ft/s). The longitudinal wave speed in an aluminum rod is 5.23 km/s (17,200 ft/s) [6]. The shear wave speed in an aluminum rod is 3.13 km/s (10,300 ft/s) [7]. The flexural wave speed in aluminum bars of the cross section corresponding to that of the lattice depends on the frequency and is tabulated in Table 2 [6]. Thus, the measured wave speed appears to be between the longitudinal wave speed and the flexural wave speed if a frequency of greater than 350 kHz is considered for the flexural wave. (The longitudinal and flexural wavelengths at 350 kHz are 1.49 cm (0.588 in) and 1.31 cm (0.515 in), respectively.)

As discussed in [8], the output signal contains many wave reflections from multiple wave paths arriving at the receiving transducer.

Output Frequency Spectrum

As discussed in [9], the frequency spectrum contains many resonances of the structure. The measured frequencies at the maximum amplitude of the output frequency spectra for waves arriving at various output locations for various input locations

are summarized in Table 3. The corresponding measured maximum amplitudes of the output frequency spectra for waves arriving at various output locations for various input locations are summarized in Table 4.

From Table 3, it is observed that the frequency at the maximum amplitude of the output spectrum generally occurs between 353 kHz and 450 kHz. The exceptions are for inputs at location A with corresponding outputs at locations S,T,U,V and inputs at location V_1 with corresponding outputs at locations A,B,C,D. Apparently, for the most distant locations, the high frequency components are attenuated and the frequency at the maximum amplitude of the output spectrum is lowered to approximately 115 kHz.

From Table 4, it is observed that the maximum amplitude of the output spectrum generally decreases with increasing transmitter-receiver distance, except for the first five bays. Fig.5 shows the logarithm (base 10) of the maximum amplitude of the output spectrum plotted versus the number of bay widths away from the input for inputs at locations A, L, V_0 and V_1. More precisely, the number of bay widths away is defined as the distance separating the vertical cross sections containing the input and output locations, normalized with respect to the bay width. For example, if the input is at location A, locations D and L_1 are defined as three bays away.

A straight line is drawn through the 110 data points in Fig.5 using linear regression, regardless of input location, except for the first five bays. The resulting correlation coefficient is 0.9186. Thus, it appears that the maximum amplitude of the

output spectrum decreases logarithmically with the number of bays away from the input, regardless of input location. Specifically, the correlation equation for the maximum amplitude of the output for a specified number of bays away from the input is

$$\mathrm{Log}_{10}\ (\text{Amplitude in mV}) = 1.10354 - 0.03690x(\text{No. of Bays}) \quad (1)$$

Eqn. (1) can be manipulated and rewritten as

$$\text{Amplitude in mV} = 12.69\ e^{-0.085x(\text{No. of Bays})} \quad (2)$$

Thus, an attenuation of the maximum amplitude of the output spectrum can be defined for LSS based on the number of lattice bays and eqn. (2). For the planar lattice structure considered, this attenuation is found from eqn. (2) to be 0.085 neper per bay. The attenuation described by nepers per bay may be convenient in the design of LSS consisting of periodic lattice bays because it is based on a natural unit of the LSS, namely, the lattice bay. It represents an insertion loss in the maximum amplitude of the output spectrum for wave propagation due to the addition ("insertion") of a periodic lattice bay.

Because the width of a bay is 6.25 cm (2.46 in) as shown in Fig. 1, the attenuation of 0.085 neper per bay can also be expressed as 0.014 neper/cm (0.035 neper/in). This compares with the longitudinal attenuation of 0.015 neper/cm (0.038 neper/in) for bulk aluminum at ultrasonic frequencies of the order of 1 MHz [10]. However, when vibrational damping data obtained for a 22-bay aluminum planar lattice at frequencies below 1 kHz [4] are used to extrapolate the attenuation [11] at frequencies of the

order of several hundreds of kHz, the predicted attenuation ranges from 10^{-7} neper/cm (2.5×10^{-7} neper/in) to 10^{-6} neper/cm (2.5×10^{-6} neper/in). Thus, it appears that the attenuation increases significantly with frequency.

<u>Observation of Reciprocity</u>

As discussed in [8], from Tables 1, 3 and 4, it is observed that when the input and output locations are interchanged, the results are very similar.

Table 5 shows various comparisons of wave propagation characteristics between the 5-bay and 22-bay planar lattices.

CONCLUSIONS AND RECOMMENDATIONS

Wave propagation characteristics of an aluminum 22-bay planar lattice structure have been considered. Two ultrasonic piezoceramic longitudinal transducers were mounted at various locations on the structure. Wave measurements were obtained by injecting an impulsive load via the transmitting transducer and recording the response via the receiving transducer. The waves injected into the structure were longitudinal waves transverse to the surface although a complex stress distribution, described by directivity functions, was actually realized [10]. The impulsive loading signal had a broad frequency spectrum containing frequencies greater than 0.5 Mhz.

Based on the results of this study, the following conclusions can be made:

(1) The measured wave speed for initial wave arrivals ranges from 4.53 km/s (14,800 ft/s) to 5.18 km/s (17,000 ft/s), which is between the longitudinal wave speed and the flexural wave speed for flexural waves of frequencies greater than 350 kHz.

(2) The output signal contains many wave reflections from multiple wave paths arriving at the receiving transducer.

(3) The measured frequency at the maximum amplitude of the output frequency spectrum generally occurs between 353 kHz and 450 kHz.

(4) The measured maximum amplitude of the output frequency spectrum decreases logarithmically with increasing number of lattice bays away from the input location, regardless of

input location on the structure, except for the first five bays.

(5) In accordance with the preceding conclusion, an attenuation of the maximum amplitude of the output spectrum can be defined for LSS based on the number of lattice bays away from the input. This attenuation may be convenient for the design of LSS because it is based on a natural unit of the LSS, namely, the lattice bay. For the planar lattice considered, this attenuation is found to be 0.085 neper per bay.

(6) As discussed in [8], reciprocity between input and output is observed experimentally.

Based on the results of this study, the following recommendations can be made:

(1) This experimental study should be extended to 3-dimensional lattice structures such as tetrahedral trusses.

(2) Scaling laws for other structural sizes, geometries, frequencies and materials should be developed; and the effects of joints on such scaling laws should be delineated.

(3) The validity of the attenuation of the maximum amplitude of the output spectrum defined based on the number of bays away from the input regardless of the input location in the LSS should be verified by considering other lattice structures.

(4) The effects of boundaries, lattice member connectivities, and structural defects on the wave speed, the frequency at the maximum amplitude of the output frequency spectrum, and the attenuation of the maximum amplitude of the output spectrum per bay should be considered.

(5) The measured initial wave speed appears to be between the longitudinal wave speed and the flexural wave speed. The exact nature of the wave mode transmission should be investigated. The possibility of wave mode conversion for waves propagating through a "T" or "L" joint should not be excluded.

(6) The possibility of a decrease in the frequency at the maximum amplitude of the output spectrum as the signal propagates should be investigated. It's effect on the attenuation of the maximum amplitude of the output spectrum per lattice bay should also be considered.

(7) For the 22-bay lattice, at the frequencies considered, the measured attenuation of the maximum amplitude of the output spectrum per bay happens to correspond closely to the longitudinal attenuation in bulk aluminum. The exact nature of this attenuation should be investigated.

(8) Reciprocity between the input and the output has been observed qualitatively. However, quantitative measures of reciprocity should be developed.

(9) Analytical efforts for predicting the output signal measured from the planar lattice should be undertaken [12-15]. Perhaps the analytical skill so developed could be extended to better understand wave propagation in three-dimensional LSS. Perhaps, statistical energy analysis (SEA) or pattern recognition techniques should also be considered in this regard.

In conclusion, this experimental study demonstrates that

wave propagation characteristics of a lattice structure can be obtained. In particular, the wave speed, the frequency at the maximum amplitude of the output spectrum, and the attenuation of the maximum amplitude of the output spectrum per lattice bay appear to be useful parameters for the characterization of wave propagation properties of LSS.

REFERENCES

[1] M.F. Card and W.J. Boyer, "Large Space Structures--- Fantasies and Facts", Proceedings of AIAA/ASME/ASCE/AHS 21st Structures, Structural Dynamics and Materials Conference, Held in Seattle, WA, May 12-14, 1980, Part 1, American Institute of Aeronautics and Astronautics, N.Y., NY, 1980, pp. 101-114.

[2] J.H. Williams, Jr., R.H. Leiler, Jr. and S.S. Lee, "Wave Propagation Through 'T' and 'L' Lattice Joints", Air Force Contractor Report, October 1984.

[3] J.H. Williams, Jr., R.A. Schroeder and S.S. Lee, "Dynamic Analysis of Two-Dimensional Lattices", Air Force Contractor Report, August 1984.

[4] D.L. Edberg, "Material Damping of Simple Structures in a Simulated Space Environment", Department of Aeronautics and Astronautics, Stanford University, Stanford, CA, January 1985.

[5] J.H. Williams, Jr., H. Nayeb-Hashemi and S.S. Lee, "Ultrasonic Attenuation and Velocity in AS/3501-6 Graphite Fiber Composite", Journal of Nondestructive Evaluation, Vol. 1, No. 2, June 1980, pp. 137-148.

[6] K.F. Graff, Wave Motion in Elastic Solids, Ohio State University Press, Columbus, OH, 1975.

[7] J. Krautkramer and H. Krautkramer, Ultrasonic Testing of Materials, 3rd ed., Springer-Verlag, N.Y., NY, 1983.

[8] J.H. Williams, Jr., J.J. Zhang and S.S. Lee, " Wave Propagation Measurements on Two-Dimensional Lattice", Air Force Contractor Report, September 1985.

[9] J.H. Williams, Jr., E.B. Kahn and S.S. Lee, "Effects of Specimen Resonances on Acoustic-Ultrasonic Testing", Materials Evaluation, Vol. 14, No. 13, December 1983, pp. 1502-1510.

[10] J.H. Williams, Jr., H. Karagulle and S.S. Lee, "Ultrasonic Input-Output for Transmitting and Receiving Longitudinal Transducers Coupled to Same Face of Isotropic Elastic Plate", Materials Evaluation, Vol. 40, No. 6, May 1982, pp. 655-662.

[11] J.H. Williams, Jr., S.S. Lee and H. Nayeb-Hashemi, "Ultrasonic Wave Propagation Loss Factor in Composite in Terms of Constituent Properties", Journal of Nondestructive Evaluation, Vol. 1, No. 3, September 1980, pp. 191-199.

[12] J.H. Williams, Jr., F.C. Eng and S.S. Lee, "Wave

Propagation and Dynamics of Lattice Structures", Air Force Contractor Report, May 1984.

[13] J.H. Williams, Jr. and H.K. Yeung, "Nondispersive Wave Propagation in Periodic Structures", Air Force Contractor Report, January 1985.

[14] J.H. Williams, Jr., H.K. Yeung and R.J. Nagem, "Joint Coupling Matrices for Wave Propagation Analysis of Large Space Structures", Air Force Contractor Report, April 1986.

[15] J.H. Williams, Jr., R.J. Nagem and H.K. Yeung, "Wave-Mode Coordinates and Scattering Matrices for Wave Propagation in Large Space Structures", Air Force Contractor Report, October 1986.

TABLE 1 Summary of Measured Wave Speeds for Initial Waves Arriving at Various Output Locations for Various Input Locations.

Output Location	Measured Wave Speed (km/s) for Input Location			
	A	L	V_C	V_1
A	*	5.04	4.67	4.70
B	6.01	5.02	4.66	4.70
C	5.12	5.04	4.67	4.68
D	5.15	5.05	4.68	4.68
E	5.14	5.06	4.71	4.66
F	5.12	5.09	4.72	4.65
G	5.12	5.12	4.77	4.62
H	5.08	5.12	4.81	4.59
I	5.05	5.18	4.78	4.56
J	5.04	5.12	4.78	4.53
K	5.02	5.90	4.74	4.70
L	5.05	*	4.73	4.69
M	4.81	5.90	4.71	4.66
N	4.79	5.12	4.69	4.64
O	4.81	5.18	4.72	4.60
P	4.63	5.14	5.03	4.54

(Continued on next page)

TABLE 1 (Continued) Summary of Measured Wave Speeds for Initial Waves Arriving at Various Output Locations for Various Input Locations.

Output Location	Measured Wave Speed (km/s) for Input Location			
	A	L	V_0	V_1
Q	4.65	5.11	4.98	4.65
R	4.65	5.08	5.06	4.72
S	4.69	5.05	4.98	4.81
T	4.71	5.05	4.93	4.98
U	4.73	4.99	5.16	4.84
V	4.71	5.00	*	4.84
A_1	4.84	4.74	4.67	4.71
B_1	4.84	4.71	4.65	4.73
C_1	4.96	4.70	4.65	4.71
D_1	4.79	4.65	4.68	4.70
E_1	4.73	4.61	4.68	4.67
F_1	4.65	4.57	4.70	4.83
G_1	4.57	4.51	4.79	4.83
H_1	4.58	4.69	4.80	4.81
I_1	4.62	4.81	4.77	4.79
J_1	4.62	4.98	4.77	4.81

(Continued on next page)

TABLE 1 (Continued) Summary of Measured Wave Speeds for Initial Waves Arriving at Various Output Locations for Various Input Locations.

Output Location	Measured Wave Speed (km/s) for Input Location			
	A	L	V_C	V_1
K_1	4.68	4.84	4.75	5.05
L_1	4.69	4.80	4.74	5.09
M_1	4.53	4.64	4.73	5.05
N_1	4.56	4.98	4.67	5.04
O_1	4.59	4.81	4.68	5.06
P_1	4.61	4.72	5.00	5.09
Q_1	4.65	4.51	5.04	5.09
R_1	4.66	4.56	5.02	5.12
S_1	4.67	4.60	5.00	5.07
T_1	4.69	4.65	4.91	4.96
U_1	4.70	4.66	5.16	5.90
V_1	4.70	4.67	*	*

* Not applicable

TABLE 2 Calculated Flexural Wave Speed in Aluminum Bars of Cross Section Corresponding to That of Lattice at Various Frequencies [6, page 143].

Frequency (kHz)	Calculated Flexural Wave Speed	
	(km/s)	(ft/s)
100	1.89	6,200
150	2.32	7,600
200	2.67	8,800
250	2.99	9,800
300	3.28	10,700
350	3.54	11,600
400	3.78	12,400
450	4.01	13,200
500	4.23	13,900

TABLE 3   Summary of Measured Frequencies at Maximum Amplitude of Output Frequency Spectra for Waves Arriving at Various Output Locations for Various Input Location.

Output Location	Measured Frequency (kHz) at Maximum Amplitude of Output Frequency Spectrum for Input Location			
	A	L	V_0	V_1
A	*	393	368	115
B	385	393	370	115
C	370	393	370	115
D	368	393	368	390
E	373	390	370	388
F	353	390	373	390
G	368	355	375	358
H	393	445	370	390
I	393	445	373	390
J	393	373	375	390
K	393	438	385	393
L	393	*	373	390
M	393	368	375	393
N	395	353	360	393
O	390	445	360	370
P	390	443	443	358

(Continued on next page)

TABLE 3 (Continued) Summary of Measured Frequencies at Maximum Amplitude of Output Frequency Spectra for Waves Arriving at Various Output Locations for Various Input Location.

Output Location	Measured Frequency (kHz) at Maximum Amplitude of Output Frequency Spectrum for Input Location			
	A	L	V_0	V_1
Q	390	355	383	370
R	386	390	358	355
S	123	375	443	358
T	123	393	450	358
U	115	393	440	360
V	115	393	*	360
A_1	443	393	368	115
B_1	443	393	370	115
C_1	448	393	368	115
D_1	358	390	368	123
E_1	370	390	413	370
F_1	368	358	368	373
G_1	353	445	368	368
H_1	390	440	368	393
I_1	390	380	3[illegible]5	393
J_1	390	445	363	393

(Continued on next page)

TABLE 3 (Continued) Summary of Measured Frequencies at Maximum Amplitude of Output Frequency Spectra for Waves Arriving at Various Output Locations for Various Input Locations.

Output Location	Measured Frequency (kHz) at Maximum Amplitude of Output Frequency Spectrum for Input Location			
	A	L	V_0	V_1
K_1	390	395	385	393
L_1	393	388	385	393
M_1	393	395	360	395
N_1	388	448	380	393
O_1	388	380	443	380
P_1	388	358	443	358
Q_1	390	443	443	355
R_1	388	443	358	360
S_1	390	390	358	373
T_1	123	393	450	360
U_1	115	393	440	360
V_1	115	393	*	*

* Not applicable

TABLE 4 Summary of Measured Maximum Amplitudes of Output Frequency Spectra for Waves Arriving at Various Output Locations for Various Input Locations.

Output Location	Measured Maximum Amplitude (mV) of Output Frequency Spectrum for Input Location			
	A	L	V_0	V_1
A	*	9.89	3.10	3.90
B	11.63	9.65	3.23	4.29
C	11.33	9.95	3.55	4.91
D	11.69	10.30	3.61	5.05
E	11.24	10.31	3.69	5.30
F	11.70	10.85	4.61	5.64
G	12.53	11.03	5.04	7.05
H	12.90	11.23	5.69	8.41
I	12.56	11.91	6.16	8.68
J	12.43	10.95	6.49	10.21
K	10.89	10.94	6.54	10.29
L	9.89	*	6.63	10.80
M	9.78	10.94	7.79	11.46
N	7.61	11.59	8.00	11.33
O	7.51	11.33	8.85	11.79
P	5.64	11.54	9.38	11.13

(Continued on next page)

TABLE 4 (Continued) Summary of Measured Maximum Amplitudes of Output Frequency Spectra for Waves Arriving at Various Output Locations for Various Input Locations.

Output Location	Measured Maximum Amplitude (mV) of Output Frequency Spectrum for Input Location			
	A	L	V_0	V_1
Q	5.26	11.41	9.96	11.24
R	4.98	10.60	10.51	10.65
S	4.10	10.25	11.24	10.25
T	3.69	10.04	11.33	10.26
U	3.25	10.09	11.57	10.14
V	2.99	9.44	*	10.14
A_1	10.39	8.98	3.08	3.46
B_1	10.39	9.24	3.13	4.15
C_1	10.48	9.80	3.30	4.29
D_1	10.53	10.20	3.66	4.59
E_1	11.20	10.39	3.83	4.[illegible]1
F_1	11.43	10.26	4.10	4.85
G_1	11.84	10.99	4.46	5.40
H_1	11.59	10.65	4.61	6.73
I_1	11.95	10.25	4.94	7.73
J_1	11.89	10.20	5.31	8.09

(Continued on next page)

TABLE 4 (Continued) Summary of Measured Maximum Amplitudes of Output Frequency Spectra for Waves Arriving at Various Output Locations for Various Input Locations.

Output Location	Measured Maximum Amplitude (mV) of Output Frequency Spectrum for Input Location			
	A	L	V_0	V_1
K_1	11.16	10.59	5.46	10.09
L_1	9.63	10.14	6.58	12.26
M_1	9.75	10.35	6.98	12.26
N_1	9.01	10.48	7.95	12.94
O_1	8.09	10.29	8.39	11.84
P_1	7.65	10.53	9.35	11.45
Q_1	6.41	10.34	10.43	11.04
R_1	5.13	10.39	10.76	11.38
S_1	5.05	10.38	11.31	11.24
T_1	4.59	9.80	11.63	11.41
U_1	3.55	9.75	11.71	11.64
V_1	3.48	10.04	*	*

* Not applicable

TABLE 5 Comparisons of Wave Propagation Characteristics Between the 5-Bay and 22-Bay Planar Lattices.

	5-Bay Lattice		22-Bay Lattice	
	From	To	From	To
Wave Speed (km/s)	4.13	5.10	4.53	5.18
Frequency (kHz)	283	355	353	450
Amplitude versus Number of Bays:				
Correlation Coefficient	0.9296		0.9186	
Attenuation (Neper/Bay)	0.3259		0.0850	
Attenuation (Neper/cm)	0.013		0.014	

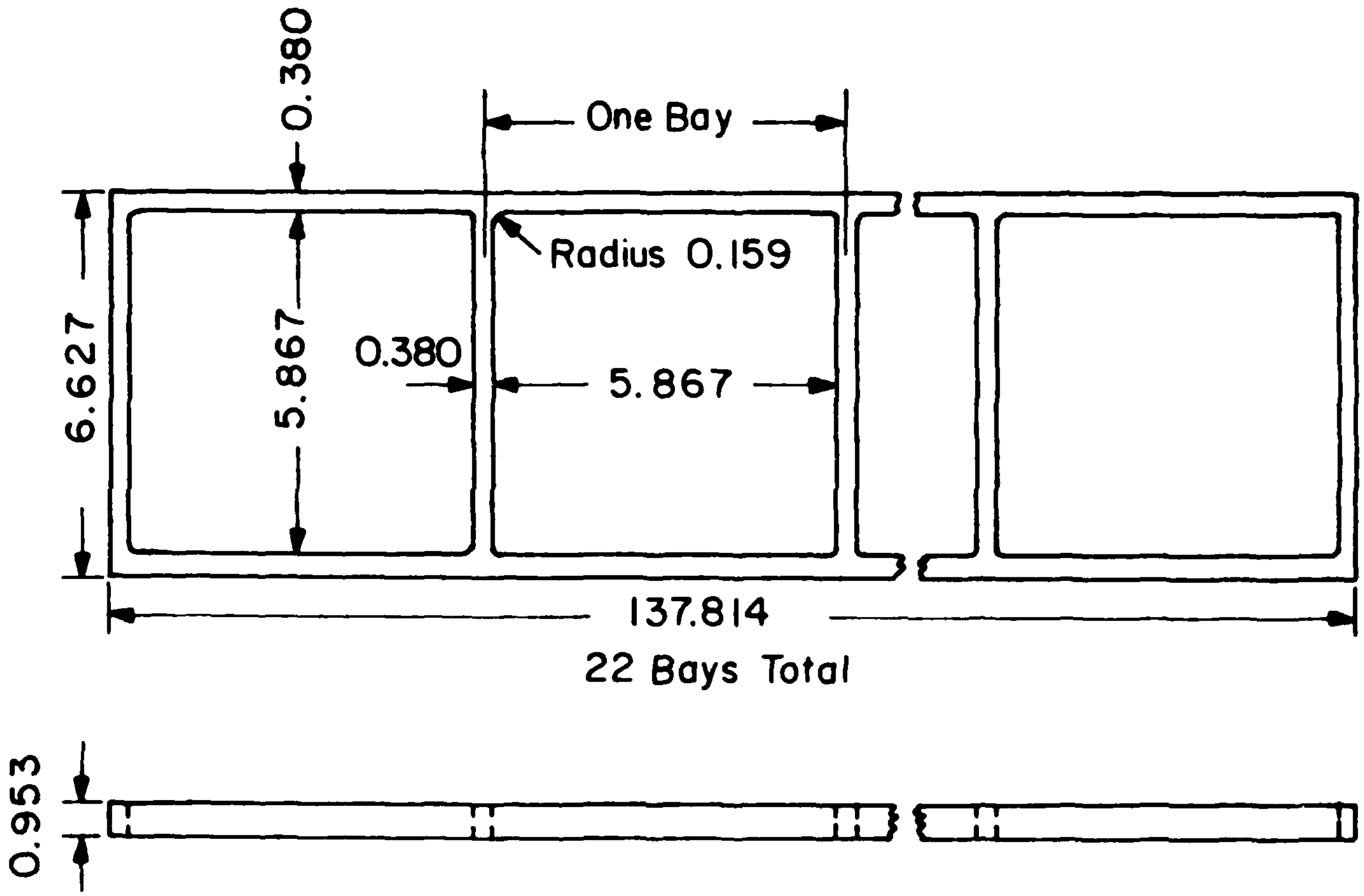

Fig. 1 Geometry of 22-bay lattice structure (dimensions in cm).

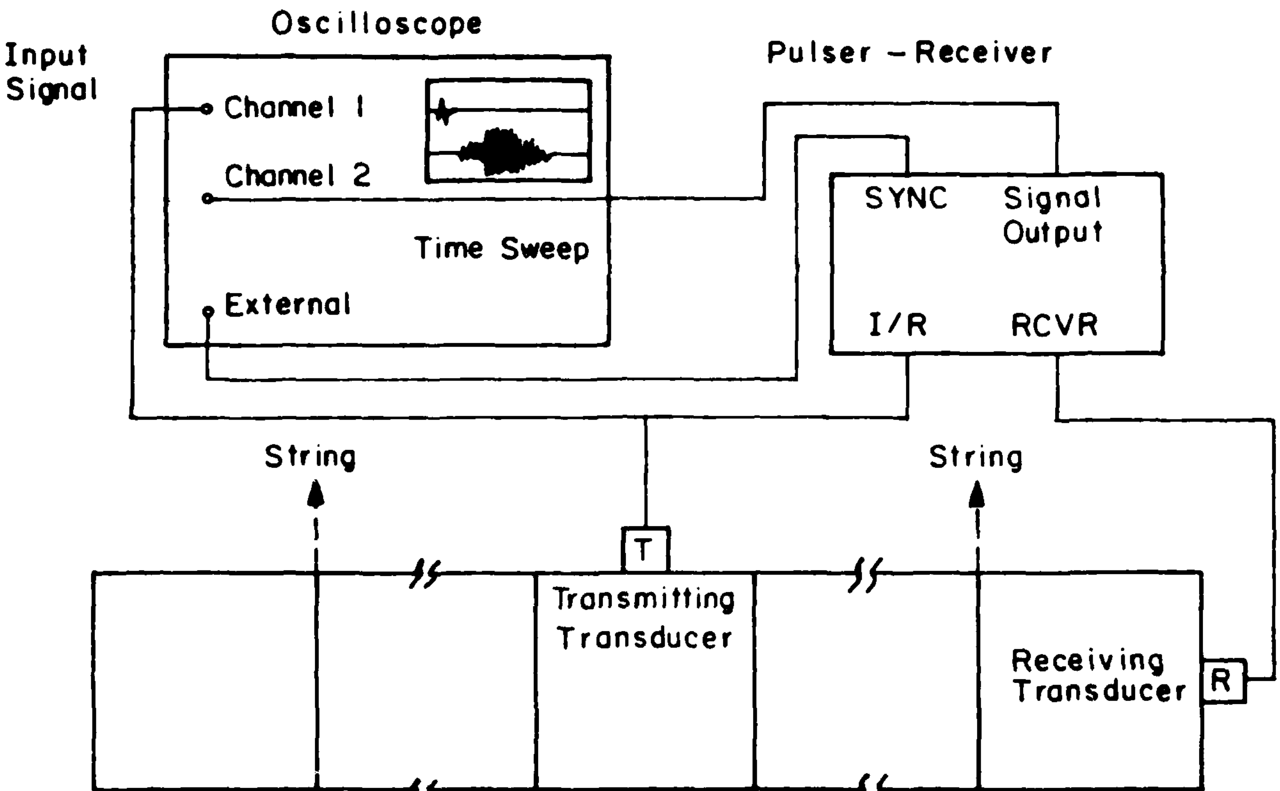

Fig. 2 Schematic of experimental system for measuring wave speed and frequency spectrum of 22-bay lattice, showing typical locations of transmitting and receiving transducers.

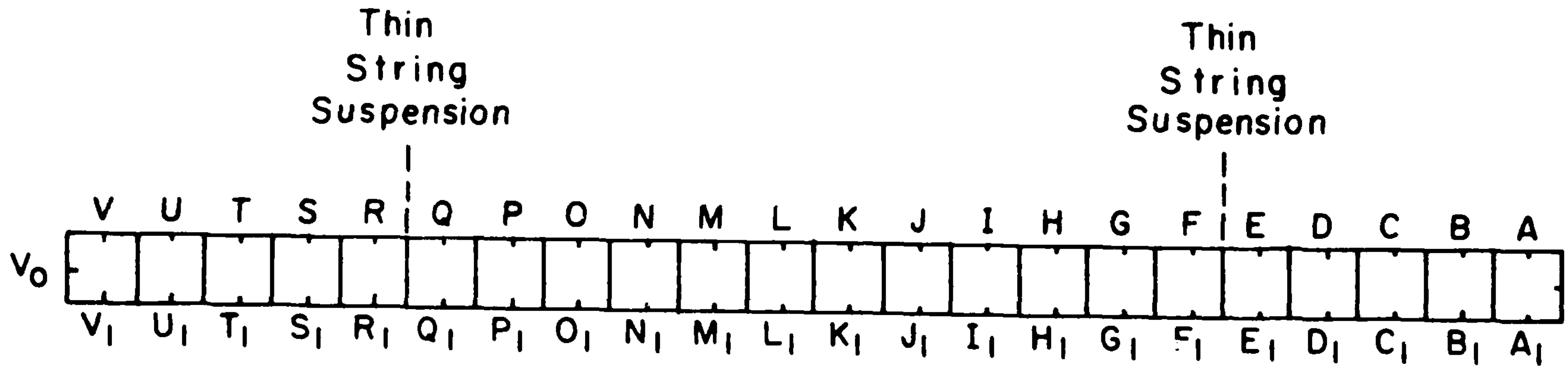

Fig. 3 Schematic illustrating locations A through V_1 on lattice structure.

(a)

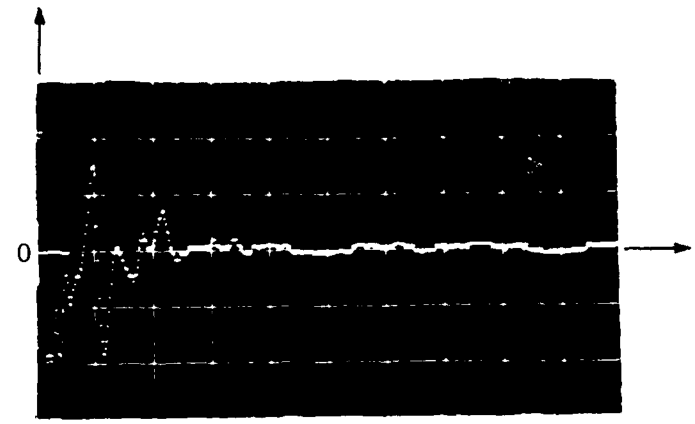

Vertical Scale:
1.00 V/Division

Horizontal Time
Sweep Rate:
9.90 μs/Division

(b)

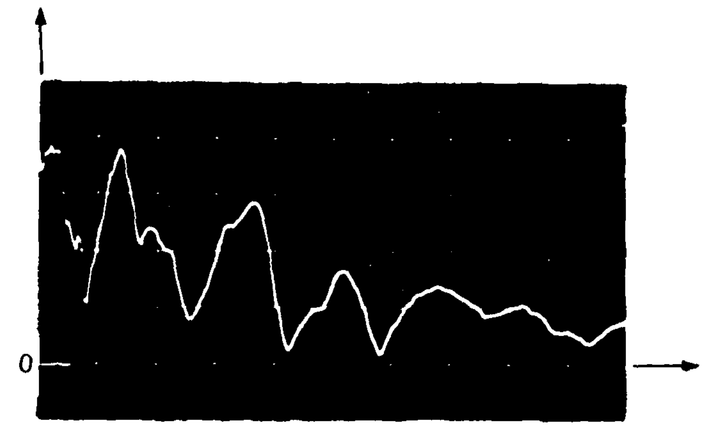

Vertical Scale:
15.63 mV/Division

Horizontal Scale:
64.00 kHz/Division

Fig. 4 (a) Time trace and (b) frequency spectrum of output from receiving transducer when transmitting and receiving transducers are coupled together directly (face-to-face) without any structural specimen.

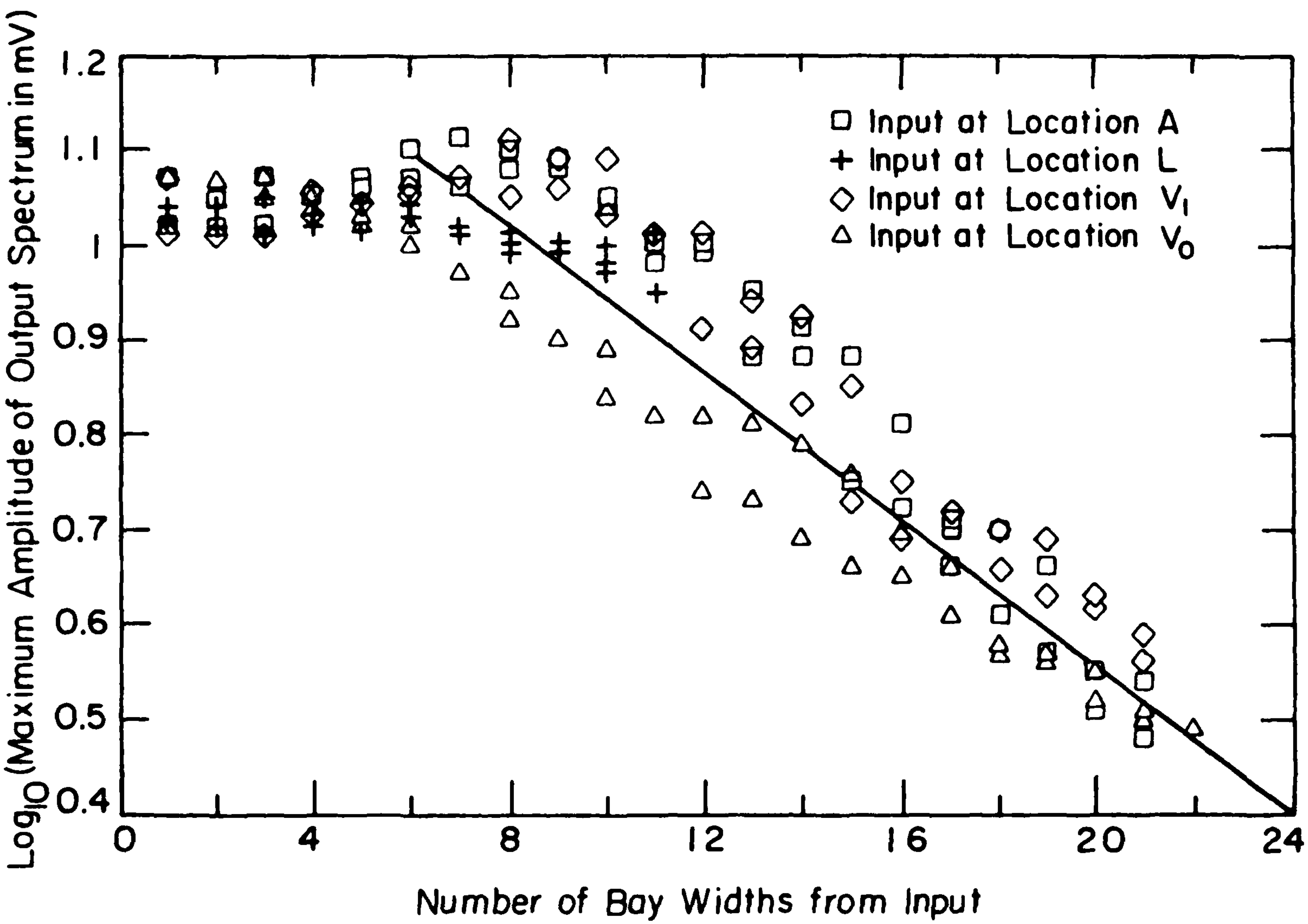

Fig. 5 Logarithm (base 10) of maximum amplitude (mV) of output spectrum versus number of bay widths that output is located from input for various input locations.

END

12-87

DTIC